Nigerian Journal of Theoretical and Environmental Physics (NJTEP)
ISSN Print: 3026-9601
ISSN Online: 1597-9849
DOI: https://doi.org/10.62292/njtep.v3i4.2025.99
Volume 3(4), December 2025

Band Gap Engineering in a Mixed Halide Perovskite $CsPbI_2Z$ (Z=F, Cl, Br) for Photovoltaic Applications

***Kwalar, B. N., Yerima, J. B. and Ahmad, A. D.**

Department of Physics, Modibbo Adama University, P. M. B. 5025, Yola Adamawa State, Nigeria.

*Corresponding author's email: bkngwani@gmail.com

Keywords:
Halide Perovskites,
Bang gap,
Density Functional Theory,
Density of States,
Quantum Espresso.

ABSTRACT

Halide perovskites are among the most promising materials for high-performance solar cells, owing to their tunable band gaps and favorable carrier transport. In this study, we apply density functional theory (DFT) with spin–orbit coupling to explore the impact of halide substitution in $CsPbI_2Z$ (Z = F, Cl, Br). Our results show that substitution systematically contracts the lattice and modifies orbital hybridization, shifting the band edges and tuning the band gap. Projected density of states analysis reveals that halide p-orbitals dominate the valence band, while Pb-p orbitals consistently govern the conduction band. Fluorine incorporation reduces the band gap from 1.45 eV to 1.40 eV, suitable for single-junction solar cells, while chlorine (1.53 eV) and bromine (1.68 eV) increase the band gap, making them attractive for tandem device configurations. All variants preserve direct band gaps at the M-point, ensuring strong light absorption. These findings establish halide substitution as a practical design pathway for optimizing $CsPbI_3$-based perovskites toward efficient and stable photovoltaic applications.

INTRODUCTION

Halide perovskites have emerged as revolutionary materials in the field of optoelectronics, attracting significant attention due to their exceptional electronic and optical properties. These materials, particularly in their mixed-halide forms, demonstrate remarkable versatility through composition- dependent property tuning (Chen *et al.,* 2021). Recent computational studies utilizing density functional theory (DFT) and first-principles approaches have systematically investigated $CsPbX_3$ systems (X = I, Br, Cl), revealing band gaps spanning from 1.37 to 3.13 eV, making them highly suitable for various optoelectronic applications (Ghaithan *et al.,* 2021).

The electronic structure of these materials exhibits fascinating characteristics, with several studies confirming the presence of direct band gaps and efficient charge transport properties (Chen *et al*., 2018). Advanced computational investigations using modified Becke-Johnson approaches with spin-orbit coupling have demonstrated that the electronic structure can be systematically modified through halide substitution (Ghaithan *et al.,* 2021). Notably, increasing iodide content leads to reduced band gaps and red-shifted absorption, while chloride substitution results in larger band gaps and blue- shifted absorption (Rajeswarapalanichamy *et al.,* 2020).

These electronic modifications are intimately connected to structural changes within the perovskite framework. Research has shown that halide substitution influences lattice volume, leads to octahedral distortions, and can trigger composition-dependent phase transitions (Chen *et al*., 2018). Some studies have reported that mixed halide compositions exhibit minimal bandgap bowing, attributed to complex interactions involving antibonding character, tilt distortions, and entropy effects (Nam *et al.,* 2023). Furthermore, pressure-dependent studies have revealed interesting phenomena, including semiconductor-to-metal transitions under high pressure conditions (Rajeswarapalanichamy *et al.,* 2020).

The stability of these materials has been a crucial focus area, with mixed halide compositions showing improved structural stability compared to their single-halide counterparts (Mikłas *et al.,* 2025). However, certain combinations, particularly mixed (I, Cl) compositions, present formation challenges below specific temperatures (Yin *et al.,* 2014). These findings have important implications for material synthesis and device fabrication.

From an applications perspective, these materials show remarkable promise across multiple technological

domains. Their tunable band gaps make them excellent candidates for solar cells, where optimized absorption characteristics can enhance power conversion efficiencies (Pandey and Chakrabarti, 2020). Additionally, their unique electronic properties make them suitable for light-emitting diodes and other optoelectronic devices (Chen *et al*., 2018). Recent computational studies using advanced DFT methods, including van der Waals functionals and ultra-soft pseudo-potentials, have revealed the formation of advantageous energy level configurations that could enhance light harvesting efficiency (Çelik, 2023).

Despite these extensive investigations, there remains a significant gap in our understanding of fluorine incorporation in $CsPbI_2Z$ systems, particularly in conjunction with other halides like chlorine and bromine. While various computational approaches have been employed to study mixed halide systems, ranging from standard DFT to more sophisticated methods incorporating spin-orbit coupling and modified exchange-correlation functionals (Ghaithan *et al.,* 2021), the specific effects of fluorine substitution remain unexplored. This study addresses this knowledge gap by investigating band gap engineering in $CsPbI_2Z$ (Z = F, Cl, Br) systems using first-principles calculations, potentially opening new avenues for material design and optimization in next-generation optoelectronic devices.

MATERIALS AND METHODS

Materials

The materials that were used in this work are as follows: Dell Laptop Latitude E6530, Quantum espresso code version 7.4.1, High Performance Computer (HPC), Internet router and Source of electricity.

Methods

Theoretical Framework

The foundation of band gap engineering in mixed-halide perovskites such as $CsPbI_2Z$ (Z = F, Cl, Br) lies in the transition from the many-electron Schrödinger equation to the tractable Kohn–Sham (KS) formalism of density functional theory (DFT). The time-independent Schrödinger equation,

$$\hat{H}\Psi(r_1,.....,r_N) = E\Psi(r_1,.....,r_N) \quad (1)$$

(where $\hat{H}$ is the Hamiltonian, Ψ is the wave function, E is the energy and r_1-------- r_N are the positions of all N electrons in the system) captures the full quantum interactions of electrons and nuclei. However, its exponential scaling renders it unsolvable for realistic perovskite systems. Hence, Hohenberg - Kohn theorems were put forth to resolve this challenge by proving that the ground-state energy is a unique functional of the electron density n(r), thereby reducing the many-body problem to a density-based description (Hohenberg and Kohn, 1964).

Building on this, Kohn and Sham (1965) introduced an auxiliary system of non-interacting electrons governed by the KS equations:

$$\left[-\frac{\hbar^2}{2m}\nabla^2 + V_{ext}(r) + V_H(r) + V_{xc}(r)\right]\psi_i(r) = \epsilon_i\,\psi_i(r) \quad (2)$$

where $V_{ext}(r)$ is the external potential acting on the electrons, $V_H(r)$ represents the Hartree potential (i.e. the classical electron–electron repulsion), ε_i is Kohn–Sham orbital for the ith electron, m is mass of the electron, $\hbar$ is reduced Planck's constant and $V_{xc}(r)$ is the exchange–correlation potential capturing many-body effects. Through iterative self-consistency, KS-DFT yields the electron density and a set of eigenvalues ε_i that provide a practical description of the electronic band structure. Although the KS eigenvalues are not rigorously quasiparticle energies, the highest occupied and lowest unoccupied levels define a KS band gap that offers meaningful insights into trends across materials (Martin, 2020).

In halide perovskites, band gap engineering emerges naturally within this framework. Substituting I^- with smaller and more electronegative halides (F^-, Cl^-, Br^-) modifies the external potential and bond lengths, inducing lattice contraction and orbital energy shifts. These changes directly reshape the KS effective potential, lowering the valence-band maximum and tuning the conduction-band minimum. The inclusion of spin–orbit coupling (SOC), crucial for heavy elements like Pb and I, further refines the band gap description.

Thus, first-principles KS-DFT calculations provide a rigorous quantum-mechanical pathway to predict how halide substitution in $CsPbI_2Z$ modulates structural parameters and electronic states, enabling precise control of the band gap for photovoltaic applications.

Computational Details

All first-principles calculations in this study were performed using the Quantum ESPRESSO (QE) simulation suite, an open-source plane-wave and pseudopotential-based package widely used for electronic-structure calculations and materials modeling within density functional theory (DFT) (Giannozzi et al., 2009; Giannozzi et al., 2017). The electronic exchange–correlation interaction was treated using the generalized gradient approximation (GGA) as parameterized by the Perdew–Burke–Ernzerhof (PBE) functional (Perdew et al., 1996), which has been shown to provide reliable structural and electronic descriptions for halide perovskites.

Projector augmented-wave (PAW) pseudopotentials from the QE PSLibrary were employed owing to their high accuracy and transferability. PAW enables a faithful reconstruction of all-electron wavefunction

behavior in the core region and allows for moderate plane-wave cutoffs while improving the representation of relativistic and spin–orbit effects which is an essential consideration for systems containing heavy atoms such as Cs, Pb, Br, and I.

Because relativistic effects strongly influence the physics of heavy-element perovskites, spin–orbit coupling (SOC) was explicitly included in all electronic-structure calculations. SOC is known to significantly modify the electronic structure of halide perovskites by reducing the band gap and altering band dispersions, which in turn affects carrier effective masses and optoelectronic performance (Koelling & Harmon, 1977; Brivio et al., 2014). Its inclusion is therefore indispensable for producing physically accurate results, particularly in Pb- and Cs-based materials.

Structural optimizations were carried out using the variable-cell relaxation (vc-relax) scheme, allowing simultaneous relaxation of lattice constants and internal atomic coordinates. Convergence was achieved when the total-energy change was below 10^{-6} Ry, the Hellmann–Feynman forces were reduced to less than 10^{-3} Ry/Bohr, and the stress tensor components were minimized to less than 0.5 kbar, ensuring that each structure reached full thermodynamic equilibrium.

To guarantee numerical reliability, systematic convergence tests were performed for both the plane-wave kinetic-energy cutoff and the Brillouin-zone sampling. An energy cutoff of 80 Ry (~1000 eV) and an 8 × 8 × 8 Monkhorst–Pack k-point grid were identified as sufficient for converging the total energy, lattice parameters, and electronic properties. These optimized values ensure that all reported results including lattice constants, band structures, and density of states are free from numerical artifacts.

RESULTS AND DISCUSSION

Crystal Structures

The crystal structure refers to the specific way in which atoms or ions are arranged in a repeating pattern within a material. This arrangement strongly determines the material's behavior, particularly its ability to absorb sunlight, generate charge carriers such as electrons and holes, and transport them efficiently to produce electricity. Figure. 1 illustrates a typical distorted perovskite (ABX_3) structure, where Cs^+ occupies the A-site, Pb^{2+} the B-site, and I^- the X-site. In this structure, corner-sharing PbI_3 octahedra play a central role in defining the material's properties.

When one of the I^- ions is replaced with F^-, as shown in Figure. 2, the lattice undergoes increased distortion due to the smaller ionic radius and higher electronegativity of F^-. This type of substitution generally improves the structural stability of the material and helps reduce unwanted ion migration, as reported by Lee et al. (2020). Figure. 3 demonstrates that substituting I^- with Cl^- also contracts the lattice, though less significantly than with F^-, suggesting a moderate level of structural reconfiguration. In contrast, Figure. 4 shows that replacing I^- with Br^- produces minimal distortion because of the similar ionic radius between Br^- and I^-, thereby preserving the cubic symmetry of the lattice and maintaining favorable properties.

In all, the degree of octahedral distortion induced by halide substitution follows the trend: $F^- > Cl^- > Br^-$. Such structural adjustments directly shape the electronic and optical behavior of perovskites, affecting key properties like their band gap and carrier mobility, as highlighted by Jeon et al. (2015).

Table 1: Optimized Lattice Constants and Unit Cell Volumes of $CsPbI_3$ and $CsPbI_2Z$ (Z = F, Cl, Br)

Material	a (Å)	b (Å)	c (Å)	Volume (Å³)
$CsPbI_3$	6.379	6.379	6.379	259.57
$CsPbI_2F$	4.831	6.321	6.321	179.12
$CsPbI_2Cl$	5.698	6.434	6.434	235.87
$CsPbI_2Br$	5.968	6.402	6.402	244.60

Table 1 presents the optimized lattice constants and unit-cell volumes for $CsPbI_3$ and the halide-substituted compounds $CsPbI_2Z$ (Z = F, Cl, Br). Replacing iodine with smaller and more electronegative halides leads to a clear lattice contraction, following the trend F > Cl > Br. Accordingly, $CsPbI_2F$ shows the strongest reduction in lattice parameters and unit-cell volume, while $CsPbI_2Br$ exhibits the least change. Quantitatively, the unit-cell volume decreases from 259.57 Å³ in $CsPbI_3$ to 179.12 Å³ in $CsPbI_2F$, with $CsPbI_2Cl$ and $CsPbI_2Br$ displaying intermediate values of 235.87 Å³ and 244.60 Å³, respectively. This contraction aligns with the smaller ionic radii of F^- (≈1.33 Å) and Cl^- (≈1.81 Å) relative to I^- (≈2.20 Å), and is accompanied by enhanced octahedral tilting and local distortions, particularly in the fluorine-substituted phase. As noted in related studies, such modifications in Pb–X bond lengths and PbX_6 octahedral geometry directly influence the orbital overlap within the Pb–X framework, thereby shifting the valence and conduction band edges and enabling systematic tuning of the band gap (Jeon et al., 2015; Lee et al., 2020).

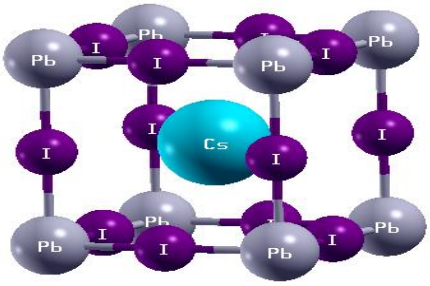

Figure 1: Crystal Structure of $CsPbI_3$

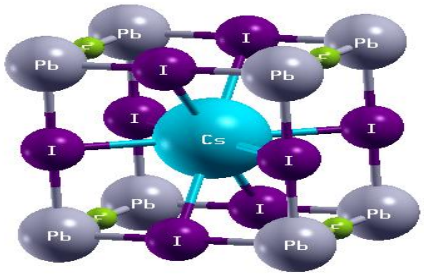

Figure 2: Crystal Structure of $CsPbI_2F$

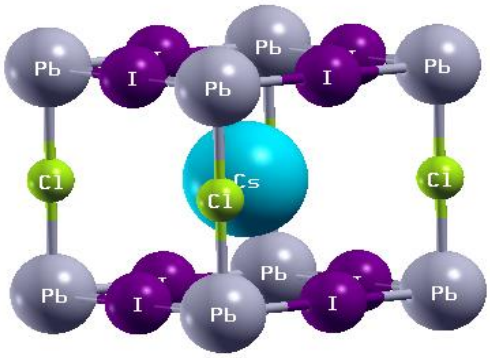

Figure 3: Crystal Structure for $CsPbI_2Cl$

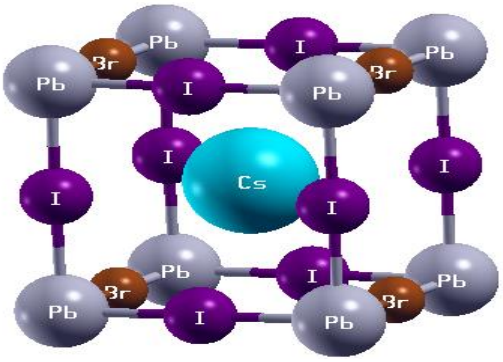

Figure 4: Crystal Structure for $CsPbI_2Br$

Electronic Properties of $CsPbI_3$ and Substituted Variants

The electronic structure calculations (DOS, PDOS and band structures) reflect the lattice trends summarized in Table 1. All four compounds retain a direct band gap at the M-point; however, the magnitude of the gap varies with halide substitution in a manner that correlates with the lattice contraction. Specifically, we obtain the following PBE+SOC band gaps: $CsPbI_3$ = 1.45 eV, $CsPbI_2F$ = 1.40 eV, $CsPbI_2Cl$ = 1.53 eV, and $CsPbI_2Br$ = 1.68 eV (see Fig. 13–16). The unusual ordering, where $CsPbI_2F$ shows a slightly *smaller* gap than pristine $CsPbI_3$ despite the strong lattice contraction, can be rationalized by analyzing the combined effects of structural distortion, orbital hybridization and spin–orbit coupling.

Electronic properties reveal the behaviors and characteristics of electrons in a material that determine how it interacts with electric fields, currents, and electromagnetic radiation. These properties are crucial in deciding whether a material behaves as a metal, semiconductor, or insulator and how well it performs in electronic or optoelectronic devices like solar cells, transistors, or LEDs. The various electronic properties are Density of States (DOS), Projected Density of States (PDOS) and Electronic Band Structures. In this section the various electronic properties of $CsPbI_3$ and its halide substituted variants were analyzed.

Density of States (DOS) of $CsPbI_3$ and Substituted Variants

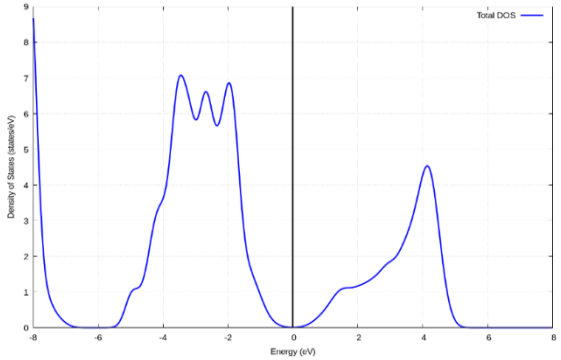

Figure 5: Density of States for $CsPbI_3$

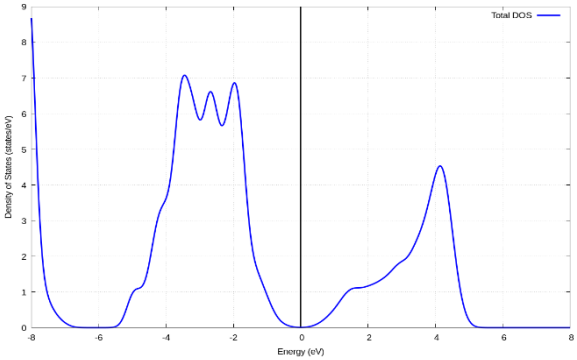

Figure 6: Density of States for $CsPbI_2F$

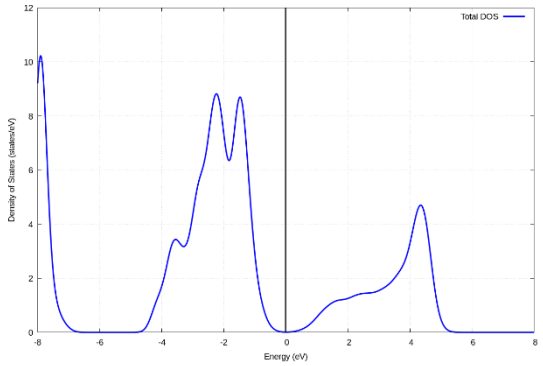

Figure 7: Density of States for $CsPbI_2Cl$

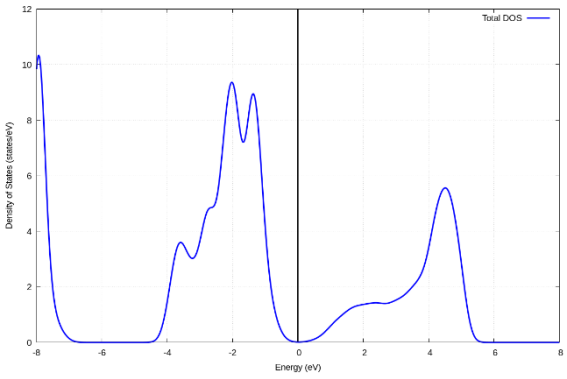

Figure 8: Density of States for $CsPbI_2Br$

The density of states (DOS) maps how electronic states are distributed across energy levels, revealing how electrons occupy and move between them. As highlighted by Afreen and Sajjanar (2025), the density of states around the valence band maximum (VBM) and conduction band minimum (CBM) plays a decisive role in semiconductors because it determines how many electronic states are available for photo-generated carriers; thereby shaping the material's absorption behavior, electrical conductivity and overall carrier lifetime. In Figures. 5 to 8, similar trend was observed in the DOS plots, the valence band has more electronic states been occupied than the conduction band around the fermi level, this shows that there are more electrons that are ready to be excited than those excited. This trend was observed for all the materials but with minimal disparity which occurred due to substitution.

Projected Density of States (PDOS) of $CsPbI_3$ and Substituted Variants

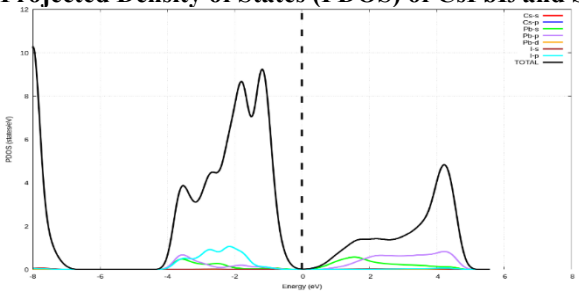

Figure 9: Projected Density of States for $CsPbI_3$

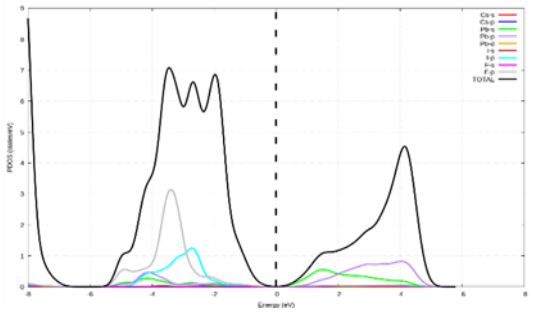

Figure 10: Projected Density of States for $CsPbI_2F$

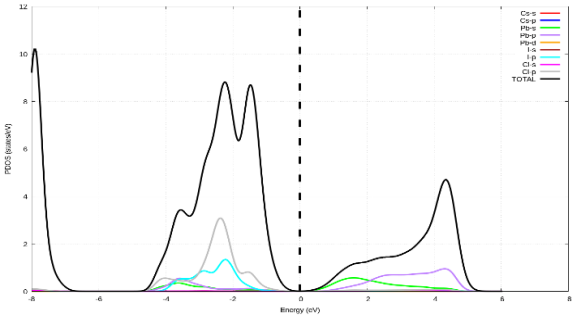

Figure 11: Projected Density of States for $CsPbI_2Cl$

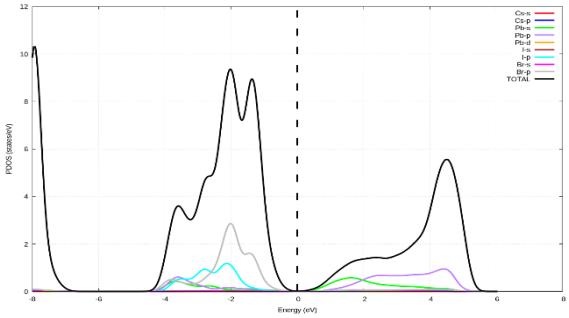

Figure 12: Projected Density of States for PbI_2Br

In Figures. 9 to 12, the PDOS results for $CsPbI_3$ and its halide-substituted forms reveal a clear and consistent pattern in their electronic behavior. In every composition, the top of the valence band maximum (VBM) is largely shaped by the p-orbitals of the halide atoms, while the bottom of the conduction band minimum (CBM) is mainly controlled by Pb-p states with a small contribution from Pb-s orbitals. This distribution of orbital character is typical of lead-halide perovskites and agrees well with earlier first-principles findings (Zhang et al., 2021). This trend is consistent with earlier findings showing that substituting iodine

with more electronegative halides systematically modifies orbital hybridization and shifts the band edges (Kumar et al., 2020).

This result fits well with the report by Zhang et al. (2019), who found that fluorine's very high electronegativity and small size cause the strongest structural distortion and orbital reshuffling, which in turn leads to unusual I-p features near the CBM and a noticeable widening of the band gap. Chlorine also lowers the VBM energy and broadens the gap, but less drastically than fluorine. This outcome is consistent with the findings of Noor et al. (2021), who noted that bromine's electronegativity and ionic size; being quite close to that of iodine cause only slight structural changes and largely maintain the original band structure.

This overall trend agrees with the observations of Yin et al. (2014) and Kumar et al. (2020), who reported that moving from I → Br → Cl → F; where electronegativity increases and ionic size decreases consistently shifts the VBM, adjusts the band-gap size and strengthens orbital hybridization. At the same time, the persistent Pb-p character at the CBM keeps the conduction bands highly dispersive across all compositions, in line with their findings.

Band Structures

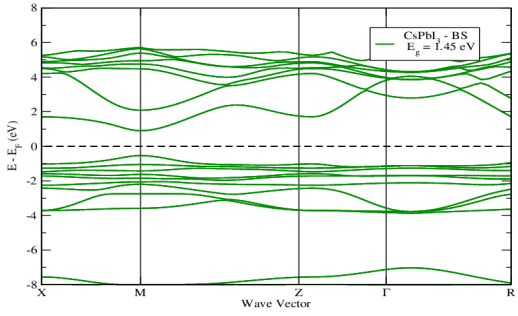

Figure 13: Band Structures for $CsPbI_3$

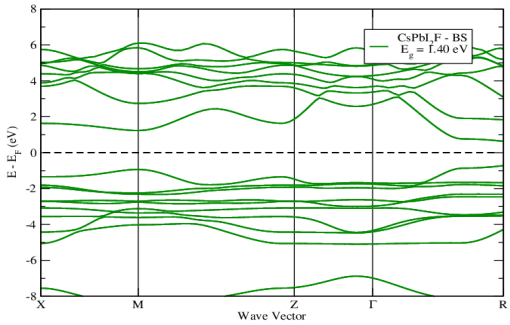

Figure 14: Band Structures for $CsPbI_2F$

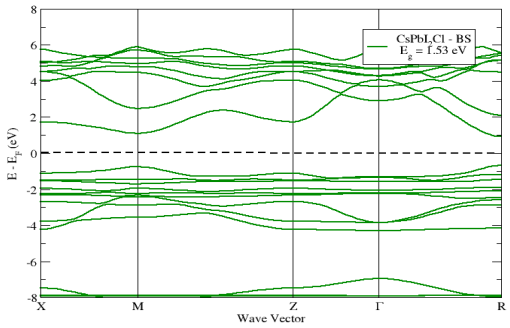

Figure 15: Band Structures for $CsPbI_2Cl$

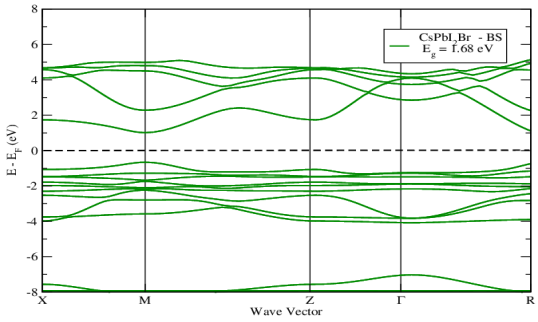

Figure 16: Band Structures for $CsPbI_2Br$

The electronic band structure of a crystal describes how electron energy varies with crystal momentum throughout the Brillouin zone. This arises from the periodic potential of the lattice, which splits electron states into allowed energy bands separated by forbidden gaps, as reported by Zhang et al. (2021). The position of the Fermi level represents the highest occupied state at absolute zero, while the band gap (E_g); the energy difference between the valence band maximum (VBM) and conduction band minimum (CBM) remains one of the most important indicators of a material's electronic and optical behavior. The Fermi level marks the highest occupied state at absolute zero and the band gap (E_g) which is the energy difference between the valence band maximum (VBM) and conduction band minimum (CBM) is key to understanding a material's performance. As noted by Cockrell et al. (2025), when the VBM and CBM fall at the same k-point, the material forms a direct band gap, making it capable of absorbing light more efficiently without needing phonon assistance which is an important advantage for photovoltaic devices. Figure. 13 - 16 show that $CsPbI_3$, $CsPbI_2F$, $CsPbI_2Cl$, and $CsPbI_2Br$ all have direct band gaps at the M-point, with valence bands having more electrons than the conduction band. This trend as observed across all the materials show a tendency of enhanced transport of charge carriers, a condition that favors device applications. $CsPbI_3$ exhibits a 1.45 eV gap, slightly below 1.63 eV; the experimental value (Xu et al., 2021), This discrepancy is expected, as GGA

functionals are known to underestimate band gaps, as reported by Leppert et al. (2019). $CsPbI_2F$ narrows to 1.40 eV, likely from doping effects, while $CsPbI_2Cl$ widens to 1.53 eV due to strong Pb–Cl bonding. For $CsPbI_2Br$, the introduction of bromine leads to a further widening of the band gap. This behavior is consistent with the larger ionic radius and modified electronic interactions introduced by Br substitution. Even with this increase, the band gaps remain well within the semiconductor range, making the material suitable for photovoltaic applications (Afreen & Sajjanar, 2025; Zhang et al., 2021).

CONCLUSION

The incorporation of fluorine reduces the band gap to 1.40 eV, making $CsPbI_2F$ well suited for single-junction solar cells operating near the Shockley–Queisser limit. In contrast, chlorine and bromine substitutions yield wider band gaps of 1.53 eV and 1.68 eV, respectively, which are advantageous for tandem architectures where wide-gap absorbers are required in the top cell. Across all systems, the consistent dominance of Pb-6p orbitals at the conduction band ensures dispersive bands and favorable carrier transport, while the halide p-orbitals govern valence band alignment, chemical stability and optoelectronic properties. It is noteworthy that material properties, including band gap, also depend on the crystal structure and space group. For example, $CsPbI_3$ in the Pnma phase, as reported by Brivio et al. (2013), has a band gap of about 1.48 eV, which compares well with the 1.45 eV obtained in our calculations. This close agreement with literature validates our computational setup and indicates that the observed band-gap reduction upon halide substitution is physically meaningful. The slight underestimation is expected, as the generalized gradient approximation (GGA) is known to underestimate absolute band gaps. On the whole, these results demonstrate that partial halide substitution in $CsPbI_3$ tunes the band gap via structural distortions and hybridization changes, producing materials with band gaps that align with photovoltaic requirements. This highlights halide substitution as a powerful design strategy to balance band-gap tuning, structural stability, and charge transport, positioning $CsPbI_2Z$ perovskites as highly adaptable, high-performance materials for next-generation solar cells

ACKNOWLEDGEMENT

The authors acknowledge the ICTP-East African Institute for Fundamental Research for the provision of computational resources.

REFERENCES

Afreen, S., & Sajjanar, S. M. (2025). Advances in Solid-State Physics: A Review of Recent Developments and Emerging Trends. *Journal of Scientific Research and Technology*. (Special Edition), 1–6.

Brivio, F., Walker, A. B., & Walsh, A. (2013). Structural and electronic properties of hybrid perovskites for high-efficiency thin-film photovoltaics from first-principles. *Apl Materials*, *1*(4).

Brivio, F., Walker, A. B., & Walsh, A. (2014). Structural and electronic properties of hybrid perovskites for high-efficiency thin-film photovoltaics from first-principles. *Apl Materials, 1*(4), 042111.

Çelik, V. (2023). Mechanism of Tunable Band Gap of Halide Cubic Perovskite $CsPbBr_{3-x}I_x$. *Sakarya University Journal of Science*, *27*(6), 1276-1285.

Chen, H., Li, M., Wang, B., Ming, S., & Su, J. (2021). Structure, electronic and optical properties of $CsPbX_3$ halide perovskite: a first-principles study. *Journal of Alloys and Compounds*, *862*, 158442.

Chen, H., Li, M., Wang, B., Ming, S., & Su, J. (2021). Structure, electronic and optical properties of $CsPbBr_{3-y}I_y$ (y = 0, 1, 2, 3) halide perovskite: a first-principles study. *Journal of Alloys and Compounds*, *862*, 158442.

Chen, X., Han, D., Su, Y., Zeng, Q., Liu, L., & Shen, D. (2018). Structural and electronic properties of inorganic mixed halide perovskites. *physica status solidi (RRL)–Rapid Research Letters*, *12*(8), 1800193.

Cockrell, C., Withington, M., Devereux, H. L., Elena, A. M., Todorov, I. T., Liu, Z. K., Shang, S. L., McCloy, J. S., Bingham, P. A., & Trachenko, K. (2025). Thermal conductivity and thermal diffusivity of molten salts: Insights from molecular dynamics simulations and fundamental bounds. *Journal of Physical Chemistry B, 129*(8), 2271–2279.

Ghaithan, H. M., Alahmed, Z. A., Qaid, S. M., & Aldwayyan, A. S. (2021). Density functional theory analysis of structural, electronic, and optical properties of mixed-halide orthorhombic inorganic perovskites. *ACS omega*, *6*(45), 30752-30761.

Giannozzi, P., Andreussi, O., Brumme, T., Bunau, O., Buongiorno Nardelli, M., Calandra, M., & Baroni, S. (2017). Advanced capabilities for materials modelling with Quantum ESPRESSO. *Journal of Physics: Condensed Matter, 29*(46), 465901.

Giannozzi, P., Baroni, S., Bonini, N., Calandra, M., Car, R., Cavazzoni, C., ... & Wentzcovitch, R. M. (2009). QUANTUM ESPRESSO: a modular and open-source software project for quantum simulations of materials. *Journal of Physics: Condensed Matter, 21*(39), 395502.

Hohenberg, P., and Kohn, W. (1964). Inhomogeneous electron gas. *Physical Review, 136*(3B), B864–B871.

Jeon, N. J., Noh, J. H., Yang, W. S., Kim, Y. C., Ryu, S., Seo, J., & Seok, S. I. (2015). Compositional engineering of perovskite materials for high-performance solar cells. *Nature*, 517(7535), 476–480.

Koelling, D. D., & Harmon, B. N. (1977). A technique for relativistic spin-polarised calculations. *Journal of Physics C: Solid State Physics, 10*(16), 3107–3114.

Kohn, W., & Sham, L. J. (1965). Self-consistent equations including exchange and correlation effects. *Physical Review, 140*(4A), A1133–A1138.

Kumar, M., Singh, R. K., & Mohapatra, S. (2020). Electronic structure and optical properties of halide perovskites: Influence of halide substitution on $CsPbX_3$ (X = I, Br, Cl). *Journal of Alloys and Compounds, 834*, 155129.

Lee, J. W., Seol, D. J., Cho, A. N.and Park, N. G. (2020). High-efficiency perovskite solar cells: recent advances and challenges. Chemical Review, American Chemical Society Publications120, 7867–7918.

Leppert, L., Rangel, T., & Neaton, J. B. (2019). *Towards predictive band gaps for halide perovskites: Lessons from one-shot and eigenvalue self-consistent GW*. Physical Review Materials, 3, Article 103803.

Martin, R. M. (2020). *Electronic structure: Basic theory and practical methods* (2nd ed.). Cambridge University Press.

Mikłas, A., Starowicz, Z., Lipiński, M., Wójcik, M. J., Nakajima, T., & Brela, M. Z. (2025). The modeling of perovskite materials $CsPbX_3$ (X= I, Br) by changing the concentration of halide: experimental and DFT study. *Physchem*, *5*(1), 3.

Nam, Y., Kim, M., Kim, S. Y., Jung, J., Kumar, G. R., Lee, J. H. and Heo, Y. W. (2023). Negligible Bowing Effect of Bandgap and Lattice Constant in a Variety of Compositions using Large Tilt Distortion in a Cesium–Lead Mixed-Halide System. *Advanced Optical Materials*, *11*(21), 2300682.

Noor, N. A., Mahmood, A., Hassan, M., & Alharthi, N. (2021). Structural, electronic, and optical properties of $CsPbX_3$ (X = Cl, Br, I) perovskites for optoelectronic applications: A DFT study. *Computational Condensed Matter, 26*, e00543.

Pandey, N., & Chakrabarti, S. (2020, April). Density functional theory based study of $CsPb(Cl/Br)_3$ mixed halide perovskites with experimental validation. In *Photonics for Solar Energy Systems VIII* (Vol. 11366, pp. 77-83). SPIE.

Perdew, J. P., Burke, K., & Ernzerhof, M. (1996). Generalized Gradient Approximation Made Simple. *Physical Review Letters, 77*(18), 3865–3868.

Rajeswarapalanichamy, R., Amudhavalli, A., Padmavathy, R., & Iyakutti, K. (2020). Band gap engineering in halide cubic perovskites $CsPbBr_{3-y}I_y$ (y= 0, 1, 2, 3)–A DFT study. *Materials Science and Engineering: B*, *258*, 114560.

Xu, S., Libanori, A., Luo, G., & Chen, J. (2021). *Engineering bandgap of $CsPbI_3$ over 1.7 eV with enhanced stability and transport properties. Science, 24*(3), Article 102235.

Yin, W.-J., Shi, T., & Yan, Y. (2014). Unusual defect physics in $CH_3NH_3PbI_3$ perovskite solar cell absorber. Applied Physics Letters, 104(6), 063903.

Zhang, C., Liu, X., & Chen, Y. (2021). *Electronic structure and orbital contributions in lead-halide perovskites: A first-principles analysis.* Journal of Materials Chemistry C, 9(14), 4756–4764.

Zhang, S., Tang, M.-C., Nguyen, N. V., Anthopoulos, T. D., & Hacker, C. A. (2021). *Wide-band-gap mixed-halide 3D perovskites: Electronic structure and halide segregation investigation*. ACS Applied Electronic Materials, 3(5), 2277–2285.

Zhang, X., Lin, H., & Liu, G. (2019). Influence of halide substitution on the band structure and stability of all-inorganic $CsPbX_3$ perovskites. *Physical Chemistry Chemical Physics, 21*(13), 6713–6720.